Semi-empirical defect calculations for the perovskite $KNbO_3$

2000 J. Phys.: Condens. Matter 12 569

(http://iopscience.iop.org/0953-8984/12/5/305)

J. Phys.: Condens. Matter **12** (2000) 569–574. Printed in the UK PII: S0953-8984(00)05716-7

Semi-empirical defect calculations for the perovskite $KNbO_3$

P W M Jacobs†‡, E A Kotomin‡§ and R I Eglitis§‖

† Department of Chemistry, The University of Western Ontario, London, ON, Canada N6A 5B7
‡ Centre for Chemical Physics, The University of Western Ontario, London, ON, Canada N6A 3K7
§ Institute of Solid State Physics, The University of Latvia, 8 Kengaraga, Riga, Latvia LV-1063
‖ Fachbereich Physik, Universität Osnabrück, Osnabrück, Germany D-49069

Received 21 June 1999, in final form 16 November 1999

Abstract. A new parametrization of the classical shell model for the cubic phase of the perovskite $KNbO_3$ has been derived and used to calculate the structural, elastic and dielectric properties of this material. Using this parametrization, the defect formation and migration energies, as well as atomic displacements, have been calculated. In parallel, the quantum mechanical method of the intermediate neglect of the differential overlap (INDO) has been applied to the same problem. The migration energies for the O vacancy obtained by these quite different methods are reasonably close (0.68 eV and 0.79 eV, respectively) and also agree with the only experimental estimate available of approximately 1 eV. Atomic relaxations calculated by these two methods agree quite well.

ABO_3 ferroelectric perovskites attract considerable attention because of their numerous technological applications [1] (particularly in optical devices) and the difficulties in modelling satisfactorily their unusual optical and dielectric properties. It is also well known that structural defects considerably affect the properties of these materials and related devices. In this paper we calculate the defect properties of $KNbO_3$ which is an important material in nonlinear optics, being used for frequency-doubling in laser applications. To this end, we combine two semi-empirical approaches—the classical SM [2] and quantum-chemical INDO [3] formalisms. The INDO approximation is a simplified version of the Hartree–Fock method which permits large-scale modelling of the atomic and electronic structure of materials; it has been successfully applied to defect calculations for many oxides, including perovskites [4]. With decreasing temperature, $KNbO_3$ undergoes a series of phase transitions from paraelectric cubic to ferroelectric tetragonal, orthorhombic, and rhombohedral phases. The displacement of Nb atoms along [100], [110] and [111] corresponds to distortions of these symmetries and thus models the transitions to the three relevant ferroelectric phases. Recently [5] the $2 \times 2 \times 2$ supercell model has been used for INDO calculations of the crystal energy of $KNbO_3$ as a function of Nb displacements along the three principal directions. Consistent with the experimental data [6], the [111] displacements provided the lowest energy minimum, and [110] the next lowest. All this is in good agreement with the first principles FP-LMTO result. The INDO parametrization developed in [5] was further checked by calculations of the atomic positions in the orthorhombic and rhombohedral phases, with results in good agreement with neutron diffraction data [6]. Calculated phonon frequencies in the cubic and rhombohedral phases also agree well with the experimental results. The INDO calculations indicate considerable covalency of the chemical bonding in pure $KNbO_3$: the effective (static) atomic charges being +0.553 for K, +2.019 for Nb, and -0.854 for O. Due to this covalency the

0953-8984/00/050569+06$30.00

analysis of the electron density distribution for the F centre (O vacancy with two electrons) [7] reveals only a small portion of the electron density to be localized inside the O vacancy (where additional sp-atomic orbitals were centred) whereas the rest of the electron density is spread out in the vicinity of the O vacancy—in contrast to conventional F-type centres in many ionic solids [4]. This result has been confirmed in first principles FP-LMTO calculations [8]. Lattice relaxation energies for atomic defects in oxides are of the order of several eV, that is about two orders of magnitude larger than the energy changes for the phase transitions. Consequently, in this discussion of defect properties we consider here only the *cubic* (high-temperature) phase of $KNbO_3$. Note that the INDO method has also been used successfully in calculations of F-type centre *migration* in MgO [9] and KCl [10]. In this paper we use the $2 \times 2 \times 2$ extended unit cell of 40 atoms, as employed earlier for the calculations on F-centres in $KNbO_3$ [7] and on Nb-impurities in $KTaO_3$ [11].

Our starting point in SM calculations was the interatomic potentials developed by Donnerberg and Exner [12] which they used to calculate defect formation energies. These Buckingham-type potentials

$$\phi_{ij}(R) = D_{ij} \exp(-R/\rho_{ij}) - C_{ij}/R^6 \tag{1}$$

where R is the distance between ions of species i and j, ϕ_{ij} is the interaction energy and i, $j = 1$ for K, 2 for Nb, and 3 for O, give reasonable defect formation energies but have the disadvantage of predicting a negative eigenvalue for the lowest transverse optic mode, which is the soft mode in $KNbO_3$. We therefore modified their potentials to fit ω_{TO1} at the Γ point in the BZ at 710 K (in the cubic phase). Moreover, we found that, as for an earlier investigation of $SrTiO_3$ [13, 14], slight adjustments in the Nb–O repulsive parameter D_{23} were all that was required to fit ω_{TO1} over the whole T-range 710–1180 K. However, we found it impossible to fit the strong temperature dependence of the static permittivity ε_s as well as that of ω_{TO1} using a conventional SM with temperature-dependent parameters.

Table 1 shows that the temperature dependence of the soft mode could be fitted successfully using a modified potential which has a K–O repulsive parameter $D_{13} = 600.3$ eV, and a temperature-dependent D_{23}. Calculated values of the static permittivity ε_s were about half the values calculated by Fontana *et al* [15], from their IR reflectance data, using the Lyddane–Sachs–Teller (LST) relation, but the calculated temperature-dependence $\varepsilon_s(T)/\varepsilon_s(T_r)$, where the reference temperature T_r is 1180 K, agreed quite closely with their values [15] for this ratio (table 1). The frequencies of the other optic modes vary hardly at all with temperature, so calculated and experimental values are compared in table 2 at just two temperatures, 710 K and 1180 K. Calculated frequencies of the Raman mode are 320 cm^{-1} at

Table 1. Temperature dependence of the lattice constant a of cubic $KNbO_3$ [15], of the Nb–O repulsive constant D_{23}, of calculated and experimental values [15] of the frequency of the soft mode, and of the ratio of the static permittivity at T, to that at $T_r = 1180$ K. Experimental values of this ratio are from Fontana *et al* [15].

			ω_{TO1} (cm^{-1})		$\varepsilon_s(T)/\varepsilon_s(T_r)$	
T (K)	a (Å)	D_{23} (eV)	Calc.	Expt.	Calc.	Expt.
710	4.0220	1332.10	96.1	96	1.92	2.00
730	4.0225	1333.00	100.2	100	1.84	1.89
803	4.0241	1334.88	106.0	106	1.65	1.67
910	4.0265	1338.00	115.7	116	1.38	1.40
1030	4.0289	1341.60	127.1	127	1.15	1.18
1180	4.0320	1345.44	136.2	136	1.00	1.00

Table 2. Comparison of frequencies of transverse and longitudinal optic modes of $KNbO_3$ calculated from the SM I (see table 3) with experiment [15].

	TO1		LO1		TO2		LO2		TO3		LO3	
T (K)	Calc.	Expt.	Calc.	Expt.	Calc.	Expt.	Calc.	Expt.	Calc.	Expt.	Calc.	Expt.
710	96	96	488	419	194	198	194	190	492	521	777	826
1180	136	136	489	418	193	204	193	194	492	511	778	815

Table 3. (a) Shell-model potentials used for $KNbO_3$ at 710 K. Buckingham repulsive (D_{ij}), hardness (ρ_{ij}) and van der Waals (C_{ij}) parameters are defined in (1). Y is the shell charge (or core charge on K^+ when it has no shell) and K is the core-shell spring constant. Potential (I) for unpolarizable K^+; (II) for polarizable K^+, $i, j = 1$ for K, 2 for Nb, and 3 for O. (b) Crystal properties calculated from potentials I and II, using the experimental lattice constant at 710 K (4.022 Å).

(a)

	ij	A (eV)	ρ (Å)	C (eV Å^{-2})	i	Y ($\|e\|$)	K (eV Å^{-2})
(I)	13	600.3	0.36198	0.0	1	1.0	—
	23	1332.1	0.36404	0.0	2	−2.811	103.07
	33	22 746.3	0.14900	27.88	3	−4.496	2100.0
(II)	The only parameters different to those in I are: $A_{13} = 640.0$ eV; $Y_1 = -2.76\|e\|$; $K_1 = 80.0$ eV Å^{-2}						

(b)

	I	II	Expt.	Ref. [12][c]
Cohesive energy (eV)	−175.52	−175.34		
Elastic constants (GPa)				
c_{11}	371	373	255[a]	398
c_{12}	116	118	80[a]	142
c_{44}	127	129	90[a]	142
Permittivities				
static ε_s	115.5	249	246[b]	516
high-frequency ε_∞	1.80	2.22	1.81[b]	1.81
Frequency of lowest transverse optic mode				
ω_{TO1} (cm^{-1})	96	69	96[b]	[d]

[a] Nunes *et al* [16].
[b] From Fontana *et al* [15]; the value of ϵ_s is the lattice contribution to ϵ_s calculated from the LST relation. Actual values measured by Yanovskii [17] are much higher due to some further polarization mechanism of unexplained origin [15].
[c] Recalculated for $a + 4.026$ Å, as used in [12].
[d] Negative eigenvalue.

710 K and 318 cm^{-1} at 1180 K, about 12% higher that the experimental value [15] of 280 cm^{-1} in the tetragonal $KNbO_3$ phase at 585 K.

The SM potentials used are given in table 3 along with calculated and experimental values of elastic constants and permittivities. Defect vacancy formation energies are compared in table 4 with the earlier calculations of Donnerberg and Exner [12]. Our modified potentials give formation energies about 3% higher for O and Nb, about 30% higher for K, perhaps indicating some special difficulties in modelling the K^+ ion. Tables 5 and 6 give the main results for the vacancy calculations using both the semi-empirical methods, SM and INDO. The atomic neighbourhood of the K and O vacancies and saddle-points are sketched in figure 1. One can see that atomic displacements agree quite closely. The SM with a polarizable K^+ ion

Table 4. Calculated vacancy formation energies for $KNbO_3$ (in eV).

	This work, potential I	Ref. [12]
a (Å)	4.022	4.026
V_O	20.44	19.68
V_K	5.76	3.99
V_{Nb}	122.83	119.57

Table 5. Atomic displacements δ around O vacancy (A) and saddle point for the migrating O_i atom (B) (in fractions of the lattice constant multiplied by 100)—see sketches in figures 1 and 2, respectively. SM stands for the shell model, numbers in brackets are results for the rigid K^+ ion potential I (table 3), q_{eff} is the effective ionic charge (in $|e|$). Outward displacements are positive, inward displacements negative; N is the number of ions equivalent by symmetry.

			SM	INDO	
	Ion	N	δ	δ	q_{eff} (e)
A	Nb	2	8.70 (8.16)	8.21	1.72
	O	8	−2.35 (−2.80)	−2.44	−0.82
	K	4	1.31 (1.11)	1.73	0.50
B	O_i[a]	1	1.54 (1.25)	1.14	−0.72
	Nb_1	1	8.50 (8.10)	7.89	+1.68
	Nb_2	2	7.40 (7.14)	7.80	+1.83
	Nb_3	1	1.06 (1.70)	fixed	+1.85
	O_1	2	1.61 (1.58)	1.30	−0.81
	K	8	2.20 (1.1)	1.52	0.50
Migration energy (eV)			0.67 (0.68)	0.79	

[a] With respect to the mid-point of the line joining the two vacancies.

results in only slightly larger K^+ displacements. The INDO effective atomic charges presented in table 5 show that: (i) charges for Nb and O are quite different from those expected in a completely ionic model (Nb^{+5}, O^{-2}, K^+) but close to those found earlier for perfect $KNbO_3$ [5], (ii) the effective charges for the *interstitial* O_i and K_i atoms are close to those for regular lattice sites, which justifies the use of the same SM potentials in migration studies as developed for the perfect crystal. The remarkable point is that a SM potential can incorporate so effectively the covalency of Nb–O bonds in $KNbO_3$. The calculated migration energies for O atoms are very similar for the SM with and without a K^+ shell, and are only smaller by 15% than the INDO value where the covalency effects are properly incorporated.

The largest displacements occur for Nb atoms which give the dominant (90%) contribution to the lattice relaxation energy. We are aware of only one experimental estimate of about 1 eV [18] for the O vacancy migration energy which agrees qualitatively with our findings. This demonstrates that O vacancies could be quite mobile in $KNbO_3$ at elevated temperatures. The INDO calculations give the activation energy for the K vacancy migration to be 0.60 eV, which is even smaller than that for the O vacancy. Unfortunately, the SM calculations were unable to locate saddle-point configurations with one imaginary eigenvalue for the migrating K^+ interstitial ion. Lastly, results of the SM calculations for the atomic displacements around Nb vacancy are also presented in table 6. We faced here the same problem in locating the saddle point, as for the K^+ ion.

In conclusion, we believe that the results presented are likely to be valid also for ferroelectric $KNbO_3$ phases as well since the atomic displacements and energy relaxations

Table 6. The same as table 5 for Nb vacancy (A), K vacancy (B), and the saddle point of the hopping K^+ ion (C) (see figure 1(a)). We were unable to find the saddle-point energy for Nb^{5+} and K^+ ions with either of the two SM potentials, in table 3.

			SM	INDO	
	Ion	N	δ	δ	q_{eff} (e)
A	O	6	11.7		
	K	8	−8.2		
	Nb	6	1.3		
B	Nb	8	−1.58 (−1.50)	−2.70	2.01
	O	12	0.73 (0.80)	0.51	−0.83
	K	6	−0.22 (−0.20)	−0.88	0.53
C	O	4		3.8	−0.83
	Nb	4		−2.5	2.01
	K	8		−0.94	0.53
	Migration energy for K^+ (eV)			0.60	

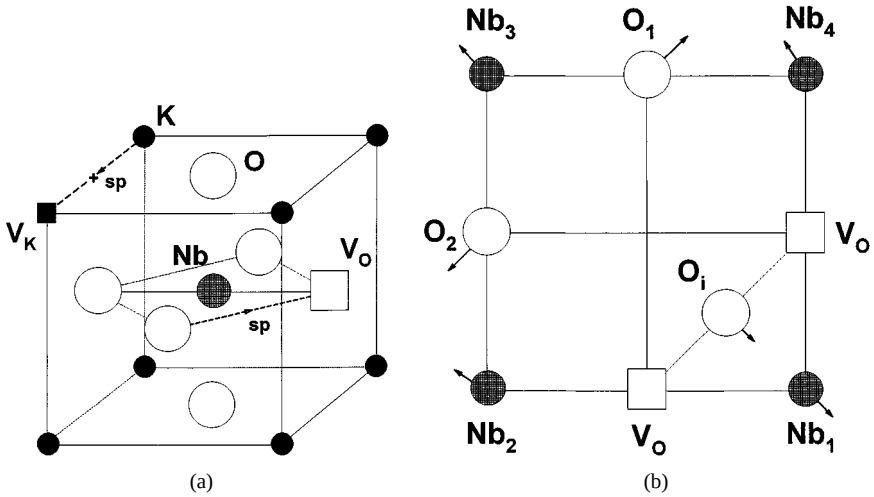

Figure 1. Unit cell of $KNbO_3$ (a) indicating saddle points (sp) for the O and K vacancy (V_O, V_K) migration paths. Displacements of atoms around interstitial O_i ion shown in sketch (b) are given in table 5.

obtained here for defects are two orders of magnitude larger than those responsible for the ferroelectric transitions [5]. It would be of great interest to check our findings with first-principles calculations, which are now in progress.

Acknowledgments

Financial support to EAK from the Centre for Chemical Physics (UWO, Canada), to RIE from the Volkswagen-Stiftung (Germany) and to PWMJ from NSERC (Canada) is greatly appreciated. We are grateful to J D Gale for a copy of his GULP code used in the SM calculatings, and to S Dorfman for stimulating discussions.

References

[1] Günter P and Huignard J-P (eds) 1998 *Photorefractive Materials and Their Applications* (Berlin: Springer)
[2] Catlow C R A and Mackrodt W C (eds) 1982 *Computer Simulations of Solids (Lecture Notes in Physics vol 166)* (Berlin: Springer)
[3] Stefanovich E, Shidlovskaya E, Shluger A L and Zakharov M 1990 *Phys. Status Solidi* b **160** 529
[4] Kotomin E A and Popov A I 1998 *Nucl. Instrum. Methods* B **141** 1
[5] Eglitis R I, Postinkov A V and Borstel G 1996 *Phys. Rev.* B **54** 2921
[6] Hewat A D 1973 *J. Phys. C: Solid State Phys.* **6** 2559
[7] Kotomin E A, Eglitis R I and Popov A I 1997 *J. Phys.: Condens. Matter* **9** L315
[8] Eglitis R I, Christensen N E, Kotomin E A Postinkov A V and Borstel G 1997 *Phys. Rev.* B **56** 8599
[9] Popov A I, Kotomin E A and Kuklja M M 1996 *Phys. Status Solidi* b **195** 61
[10] Kuklja M M, Kotomin E A and Popov A I 1997 *J. Phys. Chem. Sol.* **58** 103
[11] Eglitis R I, Kotomin E A, Borstel G and Dorfman S 1998 *J. Phys.: Condens. Matter* **10** 6271
[12] Donnerberg H-J and Exner M 1994 *Phys. Rev.* B **49** 3746
[13] Crawford J E and Jacobs P W M 1999 *J. Solid State Chem.* **144** 423
[14] Jacobs P W M 1999 *Nuovo Cimento* D **20** 1187
[15] Fontana M D, Metrat G, Servoin J L and Gervais F 1984 *J. Phys. C: Solid State Phys.* **17** 483
[16] Nunes A C, Axe J D and Shirane G 1971 *Ferroelectrics* **2** 291
[17] Yanovskii V K 1980 *Sov. Phys.–Solid State* **22** 1284
[18] Smyth DM 1994 *Ferroelectrics* **151** 115